

RF Characterization of Gigahertz Flexible Silicon Thin-Film Transistor on Plastic Substrates Under Bending Conditions

Guoxuan Qin, Jung-Hun Seo, Yang Zhang, Han Zhou, Weidong Zhou, Yuxin Wang, Jianguo Ma, and Zhenqiang Ma, *Member, IEEE*

Abstract—This letter presents fabrication of a flexible 1.5- μm -channel-length silicon thin-film transistor (TFT) on a plastic substrate with a cutoff frequency f_T of ~ 3.7 GHz and a maximum oscillation frequency f_{max} of ~ 12 GHz. Radio-frequency (RF) characterization is conducted for the flexible TFT under uniaxial mechanical bending conditions, indicating slight but notable monotonic performance enhancement with larger bending strains. Equivalent circuit model and theoretical analysis are employed to understand the underlying mechanism. Flexible gigahertz TFTs are shown to be naturally suitable for high-performance RF/microwave applications under mechanical bending (deformation) environment. This letter provides insight on designing and employing flexible gigahertz active devices.

Index Terms—Bending strain, flexible electronics, modeling, silicon nanomembrane (SiNM), thin-film transistor (TFT).

I. INTRODUCTION

FLEXIBLE electronics have been predicted a promising future for their unique characteristics of bendability, conformal attachment to irregular-shape surfaces, thinner, non-breakable, lightweight, etc.[1]. Flexible thin-film transistors (TFTs), as a specific member of them, play an important role on the new wave industry. In particular, high-performance high-speed TFTs that can be operated at the gigahertz frequency range and beyond are highly desirable because they uniquely enable wireless capability and have comparable performance with their rigid-chip counterparts, thus dramatically expand the applications of flexible electronics. Examples include active antennas, long-distance radio-frequency identifications (RFIDs), biomedical telemetry devices, foldable phased-array anten-

nas, large-area radars for remote sensing, surveillance, and space exploration applications [1]–[3]. Inorganic semiconductor nanomembranes [particularly, silicon nanomembranes (SiNMs)] are the best candidates [2]–[5] for their equivalent high mobility as bulk semiconductors and more compatible to present semiconductor industries. With the exploration of transferable single-crystal SiNMs, the development of high-frequency TFTs becomes possible. The demonstrated outstanding electrical performance of flexible monocrystalline silicon devices indicates its great potential for flexible monolithic microwave integrated systems and other applications [6]–[8]. The major advantage of flexible electronics is that they are bendable and can be used in mechanical deformation conditions. Therefore, it is essential to assess flexible devices' properties with the existence of bending strains. There are only a few reports on bending strain's influence on flexible devices [5], [9], [10] and very limited studies on TFTs [11]. These works mainly focus on the direct current or low-frequency regime. Comprehensive investigation of high-frequency characteristics of flexible RF/microwave TFTs under mechanical bending conditions is yet to report. In this letter, flexible silicon TFT with a maximum oscillation frequency f_{max} over 10 GHz is fabricated, and detailed device characteristics with different bending strains at frequencies up to 20 GHz are presented. Strain equivalent circuit model and theoretical analysis are employed to better understand the underlying mechanism. This letter shows the well capability of the flexible gigahertz TFTs operating at mechanical bending conditions.

II. DEVICE FABRICATION

First, we pattern and form the source/drain (S/D) regions with high doping concentration of $\sim 10^{20} \text{ cm}^{-3}$ on the silicon-on-insulator (SOI) wafer via high-energy and high-dosage phosphorus ion implantation followed by 950 °C annealing in furnace to achieve low resistivity and, thus, enable a high-frequency response. The effective channel length is defined by the spacing between the source and drain doping regions. The top silicon template layer is then patterned into 45- μm -width strips and etched down to the buried oxide (BOX) layer. The BOX layer is then fully etched away in a diluted 49% hydrofluoric acid (HF) solution. After thorough rinsing with de-ionized water, the silicon nanostrips are flip-transferred onto a ~ 250 - μm -thick polyethylene terephthalate (PET) substrate with a high transfer yield of $> 99\%$. Double-gate structures with SiO₂/Ti/Au stack are aligned and deposited as a gate dielectric and gate metal for TFTs on a plastic substrate. Finally,

Manuscript received October 16, 2012; accepted November 28, 2012. Date of publication January 9, 2013; date of current version January 23, 2013. This work was supported in part by the Air Force Office of Scientific Research Multidisciplinary University Research Initiative project under Grant FA9550-08-1-0337, by the Presidential Early Career Award for Scientists and Engineers under Award FA9550-09-1-0482, by the National Natural Science Foundation of China under Grant 61006061, and by the Program for New Century Excellent Talents in University. G. Qin, J.-H. Seo, and Y. Zhang contributed equally to this letter. The review of this letter was arranged by Editor A. Chin.

G. Qin, Y. Zhang, and J. Ma are with the School of Electronic Information Engineering, Tianjin University, Tianjin 300072 China (e-mail: gqin@tju.edu.cn).

J.-H. Seo, H. Zhou, and Z. Ma are with the Department of Electrical and Computer Engineering, University of Wisconsin, Madison, WI 53706 USA (e-mail: mazq@engr.wisc.edu).

W. Zhou is with the Department of Electrical Engineering, NanoFAB Center, University of Texas at Arlington, Arlington, TX 76019 USA.

Y. Wang is with Masterwork Machinery Co., Ltd., Tianjin 300400, China.

Color versions of one or more of the figures in this letter are available online at <http://ieeexplore.ieee.org>.

Digital Object Identifier 10.1109/LED.2012.2231853

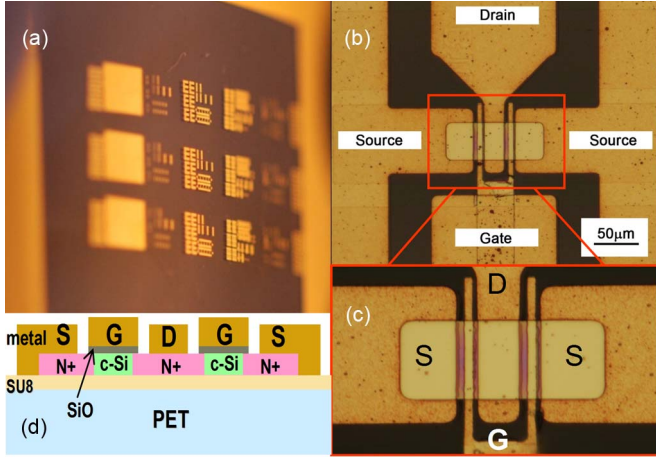


Fig. 1. (a) Optical image of the gigahertz flexible SiNM TFTs on a bent plastic substrate. (b) Optical microscope image of a finished double-gate TFT. (c) Enlarged active region of the TFT. (d) Cross-sectional schematic of the flexible double-gate TFT (drawn not to scale).

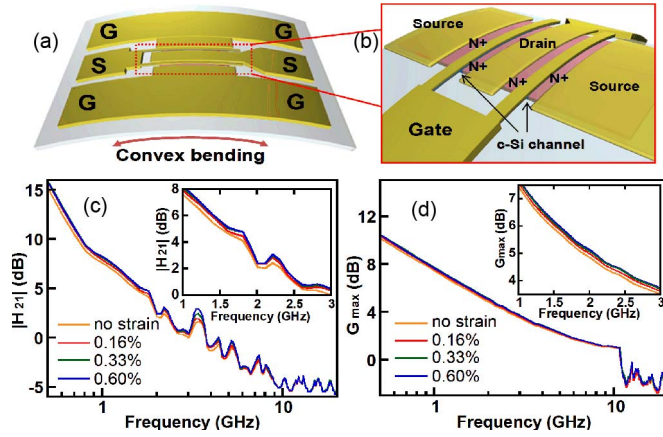


Fig. 2. (a) Illustration of the flexible TFT under mechanical bending conditions. (b) Enlarged active region. (c) Measured H_{21} (current gain) of the TFT versus the frequency with various bending strains. (d) Measured G_{\max} (power gain) of the TFT versus the frequency with various bending strains. (Insets) Clear monotonic performance enhancement with larger strains.

the S/D electrodes are formed. In particular, the S/D layout and interconnection are carefully designed to minimize the high frequency parasitics and, thus, enhance the TFT's high-frequency response. Fig. 1(a) shows the optical photo of finished TFTs on a bent plastic substrate. Fig. 1(b) shows the microscopic image of an example device (effective channel length is $\sim 1.5 \mu\text{m}$), and Fig. 1(c) shows the enlarged double-gate region. The cross-sectional schematic of the flexible SiNM TFT is also shown in Fig. 1(d).

III. RESULTS AND DISCUSSIONS

Current gain H_{21} and power gain G_{\max} are obtained from the measured S-parameters. The flexible TFT indicates a cutoff frequency f_T of ~ 3.7 GHz and f_{\max} of ~ 12 GHz (extrapolated), as shown in Fig. 2. The device shows $\sim 300 \text{ cm}^2/\text{V} \cdot \text{s}$ of electron field-effect mobility. Although with a larger effective channel length, the flexible TFT has comparable high-frequency performance with that in [6]. This is mainly because that the optimization of S/D interconnection (much wider elec-

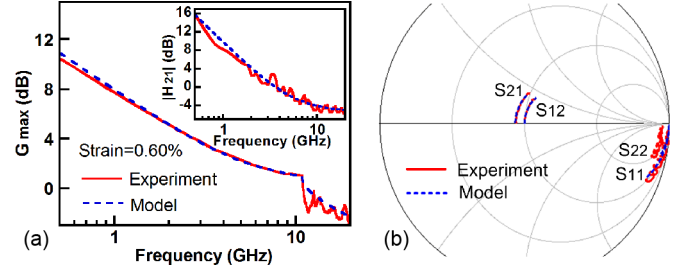


Fig. 3. Comparison of the measured (solid curves) and the calculated (dashed curves). (a) Power gain G_{\max} . (Inset) Current gain H_{21} . (b) S-parameters for the TFT, with 0.60% bending strain, as an example.

trodes and shorter interconnection) minimizes high frequency parasitics. Compared with flexible thinned MOSFETs by the backside-grinding approach [12], there are pros and cons of both fabrication methods. The approach in [12] is easier to be applied to commercial CMOS chips and fabricate devices with very small critical dimensions. While the SiNM TFTs have more flexibility and economical advantage, since the transferable nanomembranes are only ~ 250 nm thick (compared with $\sim 30 \mu\text{m}$ of thinned MOSFETs) and can be repeatedly created by making an SOI structure without grinding the Si wafer.

The flexible TFT is bended on the convex molds along the input port to the output port direction, as illustrated in Fig. 2(a) and (b). The associated tensile strains are 0.16%, 0.33%, and 0.60% (corresponds to ~ 0.7 GPa). In Fig. 2(c) and (d), the gigahertz TFT shows slight but notable monotonic performance dependence with bending strains. Both H_{21} and G_{\max} become higher with larger strains (f_T/f_{\max} are slightly increased from $\sim 3.7/12$ to $\sim 3.8/12.6$ GHz). The improvement is less than that of bulk or thinned Si MOSFETs with tensile strains [12], [13]. The major possible reasons are as follows. 1) The mobility enhancement of SiNMs with mechanical bending is less than that of bulk Si [5], [6]. In addition, for SiNM TFTs, although electron mobility will significantly influence the device performance, many other factors, particularly the deformation of evaporated SiO₂ gate dielectric layer (compared with higher quality SiO₂ dielectric layer of bulk or thinned Si MOSFETs) under bending conditions, can also affect device performance. 2) The tensile strain in this letter was uniaxial transversal (i.e., perpendicular to the channel) due to the limitation of RF probing, whereas the induced strain for bulk or thinned MOS devices is usually either uniaxial longitudinal (i.e., parallel to the channel) or biaxial. For nMOSFETs, electron mobility enhancement is stronger on the order of biaxial, longitudinal uniaxial, and transversal uniaxial tensile strains [13]. Therefore, the overall device performance improvement with tensile strain for bulk or thinned nMOS devices is larger.

To better understand the underlying mechanism, a small-signal strain equivalent circuit model is employed for the TFT device [14]. The calculated results have good agreement with the experimental results, as shown in Fig. 3. In Fig. 4, the major changing parameter source resistance R_S decreases by $\sim 14\%$ with strain up to 0.60%. The main reason is that the induced bending tensile strain increases the electron mobility of the n^+ doped regions [15], [16]; thus, the resistivity of the double sources (n^+ doped) is decreasing, leading to the smaller source resistance. To verify the speculation: 1) resistivity variations of the n^+ doped region on a same substrate are measured with

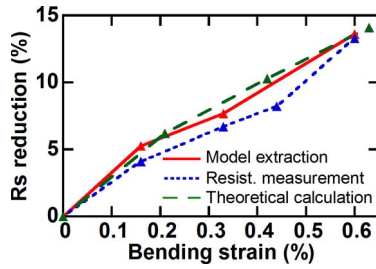


Fig. 4. Reduction of source resistance in percentage versus bending tensile strains for the gigahertz TFT (obtained by model parameter extraction, n^+ doped region resistivity measurement, and theoretical calculation, respectively).

corresponding bending strains; and 2) we calculate the R_s changes as a function of bending strains, based on mobility variations at doping concentration of $\sim 10^{20} \text{ cm}^{-3}$ with strains [16]. The results are shown together with model parameter extraction in Fig. 4, indicating good agreements between all three curves and validating the aforementioned conclusion. In addition, transconductance g_m of the flexible TFT is also an innegligible factor with tensile strains. However, due to the usage of SiNM and transversal strain as aforementioned, the mobility enhancement by mechanical bending for SiNM TFTs is less than that of bulk MOSFETs [5], [13]. Moreover, the deformation of the SiO gate dielectric layer also affects g_m and channel conductance. 1) deformation of the SiO layer induces variation to the dielectric constant of gate dielectric, since the evaporated SiO layer quality is not as good as thermally grown SiO₂ layer. In addition, deformation could also affect the effective thickness of the dielectric layer. As a result, g_m improves less. 2) Compared with the thermally grown SiO₂ dielectric layer, the evaporated SiO dielectric layer may have some pin holes (particularly by mechanical bending); thus, charges can be trapped into the dielectric layer, leading to the decreasing of g_m and the channel conductance. Consequently, the overall g_m and channel conductance enhancement are less (g_m increases $< 5\%$ at 0.6% tensile strain). According to Figs. 2 and 4, despite the physical/parameter changes, only a slight performance change is observed for the flexible gigahertz SiNM TFT. More importantly, different from the usually problematic performance variations of flexible devices [9], [10], [17], [18], the flexible gigahertz TFTs demonstrate good performance robustness under mechanical bending conditions. The results show good possibility of using the flexible gigahertz TFTs on plastic substrates for flexible MMICs under severe mechanical deformation environment without any intentional hardening.

IV. CONCLUSION

We have fabricated high-performance flexible silicon TFTs on a low-temperature plastic substrate. The 1.5- μm -channel-length TFT shows a cutoff frequency f_T of $\sim 3.7 \text{ GHz}$ and a maximum oscillation frequency f_{max} of $\sim 12 \text{ GHz}$, respectively. The TFT indicates slight but notable monotonic RF performance enhancement with larger convex bending strains. Small-signal strain equivalent circuit model and theoretical analysis are employed to understand the underlying mechanism. The results show that the flexible gigahertz silicon TFTs

are naturally suitable for high-performance RF/microwave applications under mechanical bending environment.

REFERENCES

- [1] R. H. Reuss, B. R. Chalamala, A. Moussessian, M. G. Kane, A. Kumar, D. C. Zhang, J. A. Rogers, M. Hatalis, D. Temple, G. Modell, B. J. Eliasson, M. J. Estes, J. Kunze, E. S. Handy, E. S. Harmon, D. B. Salzman, J. M. Woodall, M. A. Alam, J. Y. Murthy, S. C. Jacobsen, M. Olivier, D. Markus, P. M. Campbell, and E. Snow, "Macroelectronics: Perspectives on technology and applications," *Proc. IEEE*, vol. 93, no. 7, pp. 1239–1256, Jul. 2005.
- [2] J. A. Rogers, M. G. Lagally, and R. G. Nuzzo, "Synthesis, assembly and applications of semiconductor nanomembranes," *Nature*, vol. 477, no. 7362, pp. 45–53, Aug. 2011.
- [3] Z. Ma, "An electronic second skin," *Science*, vol. 333, no. 6044, pp. 830–831, Aug. 2011.
- [4] E. Menard, K. J. Lee, D.-Y. Khang, R. G. Nuzzo, and J. A. Rogers, "A printable form of silicon for high performance thin film transistors on plastic substrates," *Appl. Phys. Lett.*, vol. 84, no. 26, pp. 5398–5400, Jun. 2004.
- [5] J.-H. Ahn, H.-S. Kim, K. J. Lee, Z. Zhu, E. Menard, R. G. Nuzzo, and J. A. Rogers, "High-speed mechanically flexible single-crystal silicon thin-film transistors on plastic substrates," *IEEE Electron. Device Lett.*, vol. 27, no. 6, pp. 460–462, Jun. 2006.
- [6] L. Sun, G. Qin, J. H. Seo, G. K. Celler, W. Zhou, and Z. Ma, "12-GHz thin-film transistors on transferrable silicon nanomembranes for high-performance flexible electronics," *Small*, vol. 6, no. 22, pp. 2553–2557, Nov. 2010.
- [7] H.-C. Yuan, G. K. Celler, and Z. Ma, "7.8-GHz flexible thin-film transistors on a low-temperature plastic substrate," *J. Appl. Phys.*, vol. 102, no. 3, p. 034501, Aug. 2007.
- [8] Y. Sun, E. Menard, J. A. Rogers, H.-S. Kim, S. Kim, G. Chen, I. Adesida, R. Dettmer, R. Cortez, and A. Tewksbury, "Gigahertz operation in flexible transistors on plastic substrates," *Appl. Phys. Lett.*, vol. 88, no. 18, p. 183509, May 2006.
- [9] J.-H. Ahn, H.-S. Kim, E. Menard, K. J. Lee, Z. Zhu, D.-H. Kim, R. G. Nuzzo, J. A. Rogers, I. Amlani, V. Kushner, S. G. Thomas, and T. Dueñas, "Bendable integrated circuits on plastic substrates by use of printed ribbons of single-crystalline silicon," *Appl. Phys. Lett.*, vol. 90, no. 21, p. 213501, May 2007.
- [10] G. Qin, L. Yang, J.-H. Seo, H.-C. Yuan, G. K. Celler, J. Ma, and Z. Ma, "Experimental characterization and modeling of the bending strain effect on flexible microwave diodes and switches on plastic substrate," *Appl. Phys. Lett.*, vol. 99, no. 24, p. 243104, Dec. 2011.
- [11] K. H. Cherenack, N. S. Münzenrieder, and G. Troster, "Impact of mechanical bending on ZnO and IGZO thin-film transistors," *IEEE Electron Device Lett.*, vol. 31, no. 11, pp. 1254–1256, Nov. 2010.
- [12] H. L. Kao, A. Chin, B. F. Hung, C. F. Lee, J. M. Lai, S. P. McAlister, G. S. Samudra, W. J. Yoo, and C. C. Chi, "Low noise RF MOSFETs on flexible plastic substrates," *IEEE Electron Device Lett.*, vol. 26, no. 7, pp. 489–491, Jul. 2005.
- [13] K. Uchida, R. Zednik, C.-H. Lu, H. Jagannathan, J. McVittie, P. C. McIntyre, and Y. Nishil, "Experimental study of biaxial and uniaxial strain effects on carrier mobility in bulk and ultrathin-body SOI MOSFETs," in *IEDM Tech. Dig.*, 2004, pp. 229–232.
- [14] S. M. Sze, *Physics of Semiconductor Device*. New York: Wiley, 1981, p. 347.
- [15] W. Zhao, J. He, R. E. Belford, L.-E. Wernersson, and A. Seabaugh, "Partially depleted SOI MOSFETs under uniaxial tensile strain," *IEEE Trans. Electron Devices*, vol. 51, no. 3, pp. 317–323, Mar. 2004.
- [16] N. S. Bennett, N. E. B. Cowern, and B. J. Sealy, "Model for electron mobility as a function of carrier concentration and strain in heavily doped strained silicon," *Appl. Phys. Lett.*, vol. 94, no. 25, p. 252109, Jun. 2009.
- [17] G. Qin, H.-C. Yuan, G. K. Celler, J. Ma, and Z. Ma, "Influence of bending strains on radio frequency characteristics of flexible microwave switches using single-crystal silicon nanomembranes on plastic substrate," *Appl. Phys. Lett.*, vol. 99, no. 15, p. 153106, Oct. 2011.
- [18] G. Qin, H.-C. Yuan, G. K. Celler, J. Ma, and Z. Ma, "Impact of strain on radio frequency characteristics of flexible microwave single-crystalline silicon nanomembrane p-intrinsic-n diodes on plastic substrates," *Appl. Phys. Lett.*, vol. 97, no. 23, p. 233110, Dec. 2010.